TURKISH JOURNAL of ONCOLOGY

Turk J Oncol 2022;37(4):426–35
doi: 10.5505/tjo.2022.3701

ORIGINAL ARTICLE

Predictive Value of Dual-phase ^{18}F-FDG PET/CT in the Assessment of Neoadjuvant Chemotherapy Response in Patients with Locally Advanced Breast Cancer: A prospective Comparative Study with Dynamic Contrast-enhanced Magnetic Resonance Imaging

Osman KUPİK,[1] Murat TUNCEL,[2] Pınar Özgen KIRATLI,[2] Meltem Gülsün AKPINAR,[3] Kadri ALTUNDAĞ,[4] Figen BAŞARAN DEMİRKAZIK,[3] Belkıs ERBAŞ[2]

[1]Deparment of Nuclear Medicine, Muğla Training and Research Hospital, Muğla-*Türkiye*
[2]Deparment of Nuclear Medicine, Hacettepe University Hospital, Ankara-*Türkiye*
[3]Deparment of Radiology, Hacettepe University Hospital, Ankara-*Türkiye*
[4]Deparment of Oncology, MKA Breast Cancer Clinic, Ankara-*Türkiye*

OBJECTIVE

Neoadjuvant chemotherapy (NAC) is applied in locally advanced breast cancers (LABCs). Pathological complete response (PCR) after NAC is associated with prognosis. This prospective study aimed to compare the predictive value of semi-quantitative parameters obtained by dynamic contrast-enhanced (DCE) magnetic resonance imaging (MRI) and dual-phase ^{18}F-FDG PET/CT in LABC patients receiving NAC.

METHODS

Thirty-nine patients with LABC underwent DCE-MRI and ^{18}F-FDG PET/CT at baseline, and 38 after 2-3 cycles of NAC (interim). Tumor diameter, spherical volume (SV), angiographic volume, peak signal intensity (PSI), the rapid and medium component of initial rise, and percentage of Type I, Type II, and Type III curves were calculated. SUV_{max}, total lesion glycolysis (TLG), and metabolic tumor volume (MTV) were measured using adaptive (adp) and 42% thresholding methods in whole-body and late prone images. Baseline and interim studies calculated percentage changes and compared the surgery results, PCR, and non-PCR. ROC curves were obtained to calculate the area under the curve for PCR prediction. Optimal threshold values to discriminate between PCR and non-PCR were calculated.

RESULTS

Late prone images had higher sensitivity and specificity to detect the residual tumor (91%, 71.4%) than MRI (84%, 37.5%). ^{18}F-FDG PET/CT parameters differed significantly between PCR and non-PCR groups, except for MTV-42 values. Optimal cutoff values were-65% for SV%, 73% for MTV-adp%, and 88% for TLG-adp%.

CONCLUSION

Semi-quantitative parameters for ^{18}F-FDG PET/CT and volumetric changes obtained with DCE-MRI can predict response to NAC. Percentage changes in SV, MTV, and TLG can identify non-responding patients better than other parameters.

Keywords: Breast carcinoma; magnetic resonance imaging; neoadjuvant chemotherapy; positron-emission tomography dual-phase imaging.

Received: July 22, 2022
Accepted: July 26, 2022
Online: August 25, 2022

Accessible online at:
www.onkder.org

Dr. Osman KUPİK
Muğla Eğitim Araştırma Hastanesi,
Nükleer Tıp Anabilim Dalı,
Muğla-Türkiye
E-mail: osmankupik@gmail.com

INTRODUCTION

Neoadjuvant chemotherapy (NAC) is essential in treating locally advanced breast cancer patients (LABC) to reduce tumor size and stage.[1] In breast cancer patients receiving NAC, pathological complete response (PCR) is an important prognostic indicator for long-term disease-free and overall survival.[2,3] Prediction of response to NAC is critical at an early stage. In patients who do not respond to NAC, it is possible to change ineffective chemotherapy to minimize its toxic effects and prevent unnecessary costs. Successful results have been obtained in predicting the response to NAC with ^{18}F-FDG PET/CT, which evaluates the metabolic activity of the tumor. Routine PET/CT is performed in the supine position. It has been shown that dual-time imaging in the prone position contributes to evaluating primary tumors in breast cancer patients.[4-6] Dynamic contrast-enhanced (DCE) magnetic resonance imaging (MRI) of the breast is also an available method that offers high diagnostic accuracy in primary tumor therapy response assessment.[7-10]

The purpose of this prospective study was to investigate the success of dual time supine prone position ^{18}F-FDG PET/CT and DCE-MRI in predicting NAC response in patients with LABC.

MATERIALS AND METHODS

Research Ethics Standards Compliance

Our institute ethics committee approved this study (GO 13/45-29). The written informed consent form was obtained from the patients.

Study Cohort

We included patients diagnosed with LABC and planned to receive NAC. Patients Stage IIB, IIIA, IIIB, or IIIC diseases were included according to the American Joint Committee on Cancer 7th edition.[11] Patients were scanned with ^{18}F-FDG PET/CT and DCE-MRI before treatment (baseline), after 2-3 cycles of NAC (interim), and after the end of treatment, before surgery.

We did not have patients with dose infiltration, suboptimal image quality, and a feature that would prevent PET/CT or MRI. Breast cancer diagnosis in all patients was confirmed histopathologically from biopsy materials. We recorded the size of the residual tumor from the pathology results of patients who underwent a mastectomy after NAC. We accepted the absence of invasive tumor in the surgical specimen as a complete pathological response, including carcinoma *in situ*.[12-14] We grouped the patients as those with a complete pathological response (PCR) or residual tumor according to the results of the histopathological evaluation (non-PCR).

Imaging Protocol

DCE MRI and ^{18}F-FDG PET/CT have been performed sequentially within 3 days (0-6 days).

Whole-Body ^{18}F-FDG PET/CT Imaging

A dedicated PET/CT scanner (GE Medical Systems Discovery ST PET/CT scanner, LLC 3000 N, Grandview Blvd, Waukesha, Wisconsin, USA) was used for ^{18}F-FDG PET/CT imaging. All patients were requested to fast for at least 4-6 h before the PET/CT examination, and their blood glucose levels were ≤180 mg/dl before the ^{18}F-FDG injection. Patients were scanned from the skull base to the mid-thigh in the supine position, at six to seven-bed positions (3 min per bed position) with a 128×128 matrix. Iterative image processing was applied to the images (2 iterations, 21 subsets). A low-dose CT scan (4-slice, 120 kV, 300 mA) was obtained for attenuation correction and anatomic localization.

Late Prone Imaging

We produced a dense sponge material coil for PET/CT prone imaging based on the breast MRI unit's breast coil. We have optimized its dimensions so that the patient is not trapped in the PET/CT gantry. Late prone images were obtained using that breast coil. In baseline PET/CT late prone images, FDG uptake time was a median of 142 min (99-191 min), and in interim late prone images, FDG uptake time was 126.5 min (88-199 min).

MRI

MRI was performed on a 1.5 Tesla (General Electric) device using an 8-channel breast coil. Pre-contrast axial T1W (3 mm), axial (3 mm), and sagittal (4 mm) T2 fat-suppressed STIR sequences were obtained in the prone position. After intravenous administration of gadolinium contrast agent (0.5 mmol/kg), 6 times T1W (3 mm) fat-suppressed gradient echo dynamic sequences in the axial plane were obtained. After the extraction images were obtained, AngioMap and 3D reconstructed images were obtained using Computer-Aided Diagnosis (CADstream) software.

Data Analysis

Data Analysis in ^{18}F-FDG PET/CT

Visual evaluation

Two nuclear medicine physicians with over 20 years of expertise and a research assistant evaluated the images at the AW-46 workstation with a consensus. We

Turk J Oncol 2022;37(4):426–35
doi: 10.5505/tjo.2022.3701

recorded the localization and primary tumor focus and excluded patients with distant metastases.

Semi-quantitative Analysis

FDG PET/CT whole-body and late prone imaging

We calculated the tumor's SUV_{max}, SUV_{mean}, and SUL_{peak} values. Metabolic volumes (MTVs) were measured with VOI. To measure MTV, we used two different evaluation methods: The volume of the lesion measured using the threshold value of 42% of the SUV_{max} (MTV-42) and the volume of the metabolically active part of the tumor visually (MTV-adp).[15] We calculated total lesion glycolysis (TLG) using SUV_{mean} (bw)×MTVs formula. The percentage change of all measured numerical parameters after 2-3 cycles was calculated according to the following formula (% change=value after 2-3 cycles of chemotherapy-baseline/baseline value×100).

Data Analysis in MRI

Two experienced breast radiologists with over 20 years of expertise performed the visual and semi-quantitative analysis of the MRI images. Subtraction image was obtained by subtracting the images obtained before and after intravenous gadolinium. Contrast areas were detected. Tumor size, volume, and time-contrast curves were obtained using AngioMap and 3D reconstructed images using CADstream software.

Parameters Measured by MRI

(1) Number of tumors, (2) three dimensions, (3) spherical volume (SV=length × height × thickness×0.52), (4) perfusion volume (angiovolume [AV]), (5) time-contrast curves. a-Type 1-2-3 contrast enhancement percentages. b-Percentages of "rapid" and "medium" at the beginning of the contrast curve. c-PSI (PSI, maximum value of the contrast curve). The parameters change after 2-3 cycles of chemotherapy was calculated according to the formula used in PET/CT. The difference values were calculated since Types I, II, and III, and "rapid" and "medium" values were given as percentages.

Statistical Analysis

The conformity of the variables to the normal distribution was examined with the Kolmogorov-Smirnov test. Continuous variables were expressed as median (min-max) and mean with standard deviation. The parameters calculated in the whole-body and late studies were compared using parametric or non-parametric tests. As a non-parametric test, Kruskal-Wallis analysis (K-W) and Jonckheere-Terpstra (J-P) trend analysis were performed in multiple groups. Chi-square, Fisher, t-test, or Mann-Whitney U tests were used when examining the response to NAC with univariate analyses. The diagnostic decision-making properties of the calculated parameters in predicting the surgical response were analyzed by ROC curve analysis. In the presence of significant threshold values, the sensitivity, specificity, and positive and negative predictive values were calculated. $p<0.05$ was considered statistically significant. Statistical analyses were performed using SPSS 18.

RESULTS

Study Cohort

We evaluated baseline ^{18}F-FDG PET/CT images of 46 patients (mean age 46±10 years) before NAC. Two patients were excluded from the study later because they did not come for imaging after the baseline imaging. One patient died of colitis after the first course, and another patient progressed while chemotherapy was continuing. Two patients were excluded due to liver and lung metastasis. One patient did not undergo surgery voluntarily, although the imaging was completed. As a result, the data of 39 patients were analyzed to evaluate NAC response. The histopathological diagnosis of 39 patients was invasive ductal carcinoma; tumor size ranged from 22 to 120 mm (median=57 mm). PCR was observed in 12 patients (30.8%), while residual tumors were detected in 27 patients (69.2%).

The clinical data of patients are given in Table 1.

NAC Regimen

The chemotherapy regimen included four cycles of adriamycin and cyclophosphamide every 21 days, followed by weekly paclitaxel for 12 weeks. Patients with HER2+breast cancer also received concomitant weekly trastuzumab with paclitaxel.

Surgical Response Assessment

All patients underwent modified radical mastectomy following the end of NAC. The complete pathological response was detected in the primary tumor in 12 patients (30.8%). In the remaining 27 patients (69.2%), residual tumors ranging in size from 5 to 70 mm (median: 25 mm) were observed.

Visual Evaluation

^{18}F-FDG PET/CT

We evaluated the primary tumor's whole-body (n=39) and late prone (n=37) images at baseline. In 19 patients, additional tumors were detected with late prone images. After NAC, while the size and metabolic activity of the lesions decreased at different levels, no primary

Table 1 Clinical information of patients

Parameter	n	%
Hormone receptor status		
HR positive	28	72
TN	4	10
HER-2	7	18
Grade		
2	16	41
3	23	59
Menopausal status		
Pre-menopausal	26	66
Post-menopausal	13	34
T Stage		
T2	22	56
T3	14	36
T4	3	8
N stage		
N0	3	8
N1	20	51
N2	4	10
N3	12	31
Tumor focality		
Unifocal	30	77
Multifocal/multicentric	9	23

HR: Hormone receptor status; TN: Triple negative; HER-2: Human epidermal growth factor receptor-2 status

tumor was observed in whole-body images in six patients and late images in three patients. In one patient, the metabolic activity of the tumor increased. Two unifocal and one multifocal tumor not observed in whole-body images were detected in three patients with late images. We performed whole-body imaging in 34 patients at the end of NAC. Late images were present in 32 patients. While the residual tumor was observed in 19 patients with whole-body images, the residual tumor was detected in 24 patients with late images. Compared with the surgical response, the sensitivity, specificity, and positive and negative predictive values of whole-body imaging and late prone imaging were 62.5% versus 91.3%, 80% versus 71.4%, 62.6% versus 91.3%, and 47% versus 62.5%, respectively. While the highest sensitivity and positive and negative predictive values were obtained in late images, the specificity value was high with whole-body images detecting residual tumors.

Contrast-enhanced Dynamic MRI

Baseline DCE-MRI was obtained in 39 patients. While a single tumor focus (57 mm [17-200 mm]) was observed in 60% of the patients, two tumor foci were observed in 35%, and more than 2 tumor foci were observed in 5% of the patients. A significant reduction in tumor size was observed in the interim study (32 mm [5-100 mm]) ($p<0.0001$), and the major focus disappeared in one of the patients with two tumor foci. After NAC, the primary lesion completely disappeared in seven patients, while the lesion size (27 mm [11-85 mm]) decreased significantly in other patients. According to the surgical outcome, the sensitivity, specificity, and positive and negative predictive values of MRI for residual tumors were 84%, 37.5%, 80.7%, and 42.8%, respectively, Figure 1.

Quantitative Evaluation

^{18}F-FDG PET/CT

Interim images of 38 patients were evaluated. The % change values between the interim and baseline images are given in Table 2.

Response to NAC

When the % changes were compared to surgical response, %TLG-adp and % MTV-adp were significantly different according to surgical response in the whole-body and late images. These values showed more variation in the group with the complete surgical response. We found no difference in whole-body and late prone images for %MTV-42.

DCE MRI

Interim MRI was performed on 38 patients. Baseline and interim MRI parameters were not significantly different between receptor subgroups and grades. When the PCR and non-PCR groups were compared, rapid ($p=0.044$), medium ($p=0.044$), and peak ($p=0.034$) values were statistically different and changed on baseline MRI. Long diameter ($p=0.035$) and volume ($p=0.02$) in interim MRI were significantly lower in the PCR group. MRI parameters changes are given in Table 3. When the % change values calculated in 34 patients were compared according to the surgical response, long diameter ($p=0.041$), volume (0.001), and curve peak (0.03) showed more changes in the PCR group compared to the non-PCR group, Figure 2.

Predictive Value of Parameters

Between the interim and baseline studies, percent change values of PSI and SV from MRI, SUL_{peak}, MTV-adp, and TLG-adp from PET/CT could predict PCR with high accuracy. The list of parameters for which ROC analysis was performed to evaluate NAC response and whose p-value was significant is given in Table 4. In addition, the sensitivity, specificity, positive and negative predictive values, and accuracy values calculated for the determined threshold values are given in the same table (Table 4).

Turk J Oncol 2022;37(4):426–35
doi: 10.5505/tjo.2022.3701

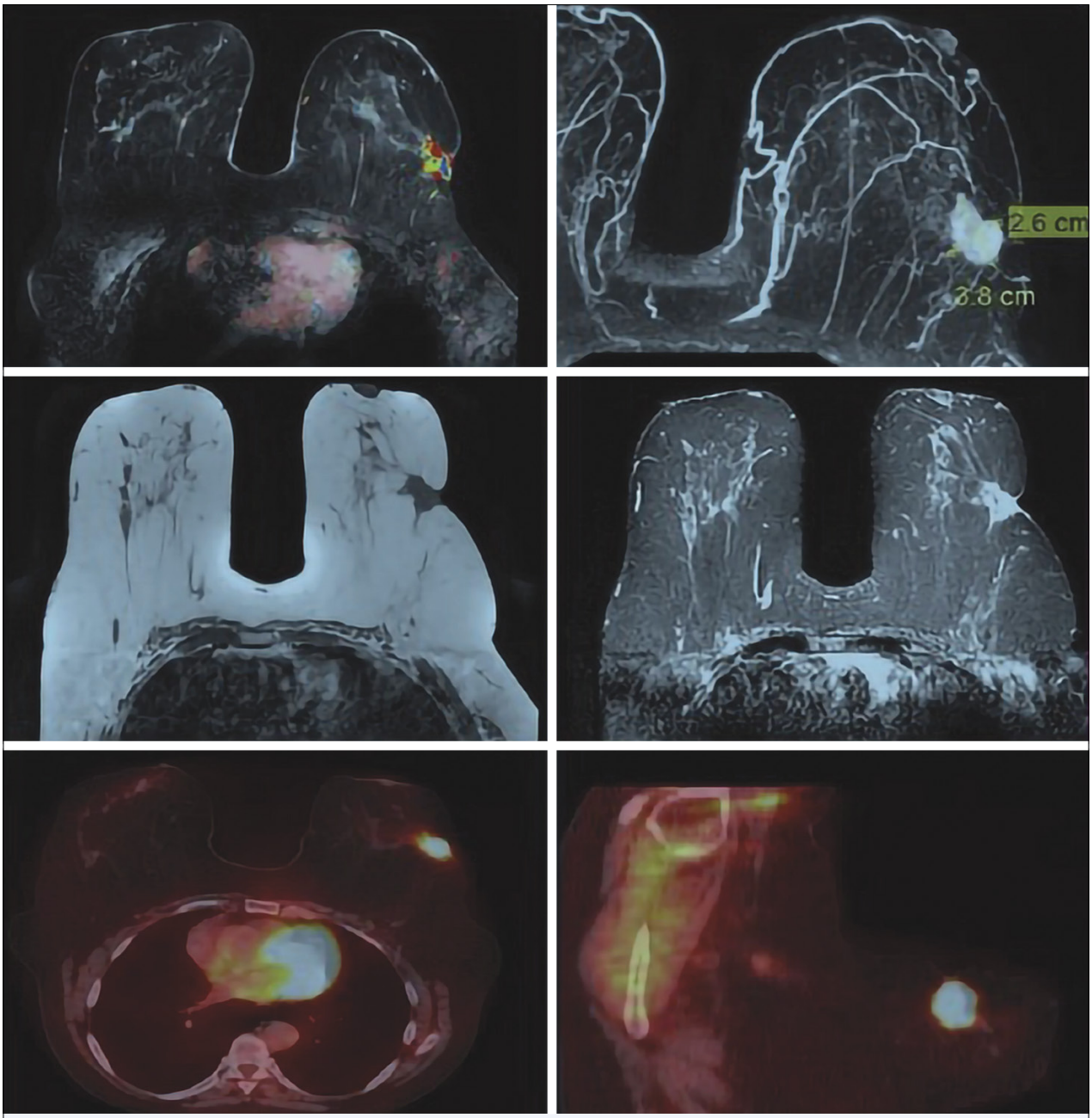

Fig. 1. Sixty-six years old, left breast invasive ductal carcinoma, Grade 2, non-luminal tumor, tumor dimensions on MRI 38×16×29 mm, spherical volume: 9.1 cc, angiovolume: 9.4 cc, peak signal intensity: 187 (upper and middle row), SUV_{max}: 14.4 (bottom row).
MRI: Magnetic resonance imaging.

DISCUSSION

This study compared ^{18}F-FDG PET/CT and DCE-MRI parameters in predicting NAC response in patients with LABC. We compared baseline, after the second or third cycle of NAC, and at the end of NAC, pre-surgical imaging, and histopathological results.

When comparing standard whole-body imaging with late prone imaging in the visual evaluation of ^{18}F-FDG PET/CT, we found that the assessment of primary tumor was most successfully performed with late prone images. The breast was evaluated more easily in the prone position using a breast coil. We detected additional primary lesions in late imaging due to the

Table 2 Percent change values of ^{18}F-FDG PET/CT parameters between interim and baseline imaging in PCR and non-pCR patients (n=38)

Parameter (% change)	Imaging	Whole patients	Patients with pCR	Patients with non-pCR	p
SUV_{max}	Whole body	-65.4 (-100, 9.3)	-90.17 (-100, -26.65)	-53.42 (-100, 9.3)	0.012
	Late prone	-62.61 (-100, 34.21)	-81.38 (-100, -36.92)	-57.77 (-100, 34.21)	NS
SUV_{mean}	Whole body	-53.45 (-100, 22.03)	-84.77 (-100, -33.59)	-41.28 (-100, 22.03)	NS
	Late prone	-55.06 (-100, -0.34)	-68.30 (-100, -25.08)	-48.18 (-100, 36)	NS
SUL_{peak}	Whole body	-64.72 (-100, 5.56)	-88.61 (-100, -44.22)	-63.23 (-100, 5.56)	0.047
	Late prone	-64.91 (-100, 0)	-83.29 (-100, -41.36)	-61.11 (-100, 0)	0.015
MTV-adp	Whole body	-63.57 (-100, -8.2)	-82.97 (-100, -23.46)	-60 (-100, -8.2)	0.03
	Late prone	-64.32 (-100, 16.59)	-83.3 (-100, -51.44)	-62.2 (-100, -16.59)	0.027
MTV-42	Whole body	5.66 (-100, 1500)	-60.51 (-100, 1500)	27.78 (-100, 369)	NS
	Late prone	-2.58 (-100, 1471)	38.89 (-100, 1185.7)	19.45 (-100, 1471)	NS
TLG-adp	Whole body	-81.61 (-100, 11.11)	-97.79 (-100, -55.76)	-80.22 (-100, 11.11)	0.004
	Late prone	-82.63 (-100, -3.06)	-95.86 (-100, -58.7)	-81.66 (-100, -3.06)	0.025
TLG-42	Whole body	-63.51 (-100, 113.19)	-90.07 (-100, -73.02)	-49.01 (-100, 113.19)	0.038
	Late prone	-60.78 (-100, 243.75)	-77.47 (-100, 243.75)	-50.36 (-100, 175)	NS

PCR: Complete pathological response; non-PCR: Non-pathological complete response; SUL_{peak} corresponding to the highest possible mean value of a 1 cm^3 spherical volume of interest (VOI); MTV-adp: Metabolic tumor volume with adaptive SUV_{max} threshold method; MTV-42: metabolic tumor volume with 42% SUV_{max} threshold method; TLG-adp: Total lesion glycolysis with adaptive SUV threshold method; TLG-42: Total lesion glycolysis with 42% SUV threshold method; NS: Non-statistically significant

increase in ^{18}F-FDG uptake in the tumor with time, the decrease in the level of ^{18}F-FDG in the normal breast tissue, and the increase in the tumor/ground activity contrast. In primary tumor evaluation, prone imaging is recommended to increase ^{18}F-FDG PET/CT sensitivity. Other authors have also described the use of breast coils which are also used to fuse MRI/PET images to increase the specificity of MRI images.[6,16] Late prone ^{18}F-FDG PET/CT images were more compatible with MRI. It is known that the late component of dual imaging increases not only specificity but also sensitivity, and our finding is consistent with the literature.[4,17]

While different tumor metabolic activity reduction levels were observed with interim ^{18}F-FDG PET/CT, we detected a reduction in lesion size with MRI. When the post-NAC, pre-surgery, ^{18}F-FDG PET/CT, and MRI images were compared with the histopathological results, the sensitivity of MRI was higher than that of whole-body supine ^{18}F-FDG PET/CT images. However, late images were more successful than MRI. Positive predictive values were higher than negative predictive values.

It is known that quantitative parameters are more successful than visual evaluation. The changes in SUV_{max} values were examined most frequently in the studies.[18-20] TLG and MTVs changes have been used.[21,22] In some of the studies, the predictive value of TLG was reported to be higher than SUV_{max} values.[22] On the other hand, while a study reports that SUV_{max} change is a more significant predictor than TLG change, a study also says that both MTVs changes are equally successful.[21,23] The % TLG-adp and %MTV-adp values showed significant differences between the PCR and non-PCR groups in whole-body and late images. No statistically significant difference was found with %MTV-42. We found the "adapted" method superior to the method in which 42% was used as the threshold value. In the literature, parameters are generally used to predict NAC response. In this study, we also examined TLG and MTV differently. In a meta-analysis of 19 articles and 920 patients, the sensitivity of PET/CT was 84%, the specificity was 66%, the positive predictive value was 50%, and the negative predictive value was 91%.[24] In the articles in this meta-analysis, the sensitivity ranged from 33% to 100%, while the specificity values were reported between 30% and 100%. In another meta-analysis, which included 745 patients and evaluated 15 studies, the values were 80.5%, 78.8%, 79.8%, and 79.5%, respectively.[25] Values ranging from 40% to 88% in SUV_{max} have been reported to predict NAC in these studies. One of the reasons why different values were detected is that imaging timing for the prediction of NAC response is not standard. Some authors imaged after one cycle, while others imaged after 2 or

Turk J Oncol 2022;37(4):426–35
doi: 10.5505/tjo.2022.3701

Table 3 Percent change values of MRI parameters between interim and baseline imaging in PCR and non-pCR patients (n=38)

Parameter	Imaging	All patients	Patients with PCR	Patients with non-PCR	p
Long diameter (mm)	Basale	57 (16. 120)	44 (25 100)	67 (16. 120)	NS
	Mid	32 (0-100)	23.5 (8, 80)	45 (0, 100)	0.035
	% Change	-21.4 (-100, 32.1)	-39.75 (-82, -10.7)	-18.85 (-100, 32.1)	0.041
Spherical volume (mL)	Basale	30.7 (1.1, 337)	27.8 (5.7, 234)	34.15 (1.1, 337)	NS
	Mid	8.9 (0.381.8)	3.29 (0.1, 61.7)	16.41 (0. 381.8)	0.02
	% Change	-52.9 (-100, 266.9)	-85.43 (-99.7, -44.2)	-49.315 (-100, 266.9)	0.002
Angiovolume (mL)	Basale	10.7 (0.2, 141)	14.9 (3.8, 45.8)	10.1 (1.0, 141)	NS
	Mid	1.5 (0, 66.2)	1.3 (0.3, 17.4)	1.6 (0.1, 66.2)	NS
	% Change	-83 (-100, -3.5)	-92.89 (-96.9, -7)	-80.54 (-97.9, -3.5)	NS
Contrast type 1 (%)	Basale	40 (6, 128)	26 (6, 89)	40 (6. 98)	NS
	Mid	60 (12, 100)	48 (16, 83)	65 (12, 100)	NS
	% Change	19 (-100, 87)	20 (-33, 74)	18.5 (-44, 87)	NS
Contrast type 2 (%)	Basale	33 (2, 74)	33.5 (11, 74)	36 (2, 72)	NS
	Mid	26 (0, 59)	33 (18, 50)	26 (0, 59)	NS
	% Change	-8 (-64, 32)	-3 (-37, 7)	-10.5 (-64, 32)	NS
Contrast type 3 (%)	Basale	13 (0, 70)	23.5 (0, 70)	10 (0, 67)	NS
	Mid	4 (0, 54)	19 (0, 34)	3 (0, 54)	NS
	% Change	-4 (-70, 26)	2 (-70, 26)	-4 (-52, 14)	NS
Medium (%)	Basale	11 (0, 91)	4 (0, 36)	14 (0, 91)	0.045
	Mid	38 (0, 100)	52 (17, 97)	37 (0, 100)	NS
	% Change	15 (-43, 91)	34 (-16, 91)	9 (-43, 62)	NS
Rapid (%)	Basale	89 (9, 100)	96 (64, 100)	86 (9, 100)	0.045
	Mid	62 (0, 100)	48 (3, 83)	63 (0, 100)	NS
	% Change	15 (-43, 91)	-34 (-91, 16)	-9 (-62, 43)	NS
Peak signal intensity (%)	Basale	243 (105, 1347)	300 (249, 362)	198 (105, 1347)	0.007
	Mid	161 (68, 695)	150 (103, 297	180 (68, 1202)	NS
	% Change	-18 (-86.3, 96.3)	-51.36 (-59, -7.2)	-13.7 (-86.3, 96.3)	0.03

MRI: Magnetic resonance imaging; PCR: Pathological complete response; non-PCR: Non-pathological complete response/residual disease; NS: Non-statistically significant

3 cycles. For ease of comparison, we studied after 2-3 cycles, which is the most frequently used time in our study. Contrary to this, Humbert et al.[26] suggested that a SUV_{max} <2.1 after the first cycle had an accuracy of 76%. The heterogeneity of the groups in the studies, the differences in PET/CT imaging times, and the lack of many patients lead to different results.

The volume change measured in standard MRI has been defined as a sensitive parameter in predicting NAC response. The contrast enhancement curve and dynamic parameters obtained by dynamic MRI with contrast provide information about the angiogenesis of the tumor. A study comparing MRI and ^{18}F-FDG PET/CT in TN and non-TN breast tumors found that MRI enhancement kinetics and SUV_{max} change were correlated. It was emphasized that MRI measured angiogenesis/perfusion and PET measured metabolism were correlated, which was more robust in the more aggressive TN group.[27] In a study comparing MRI and PET/CT, Pengel et al.[28] found the % SUV_{max} and tumor diameter change to be equally successful in predicting NAC. However, when analyzed according to receptor subgroups, the diameter change was significant only in the TN group, while the SUV_{max} change was significant in the TN and luminal groups. Using SUV_{max} and MRI enhancement parameters together, Lim et al.[29] showed that the combined enhancement curve (at least 6%) and SUV_{max} (at least 41%) change after one cure is a successful predictor of disease-free survival. A study comparing PET and MRI reported that both methods were not sensitive enough but had high specificity. SUV_{max}, SUL_{max}, SUL_{peak}, and TLG parameters of FDG PET/CT, and enhancement parameters of MRI were compared. While TLG did not differ between groups according to surgical response, SUV values differed; only SUV_{max} change was determined as an inde-

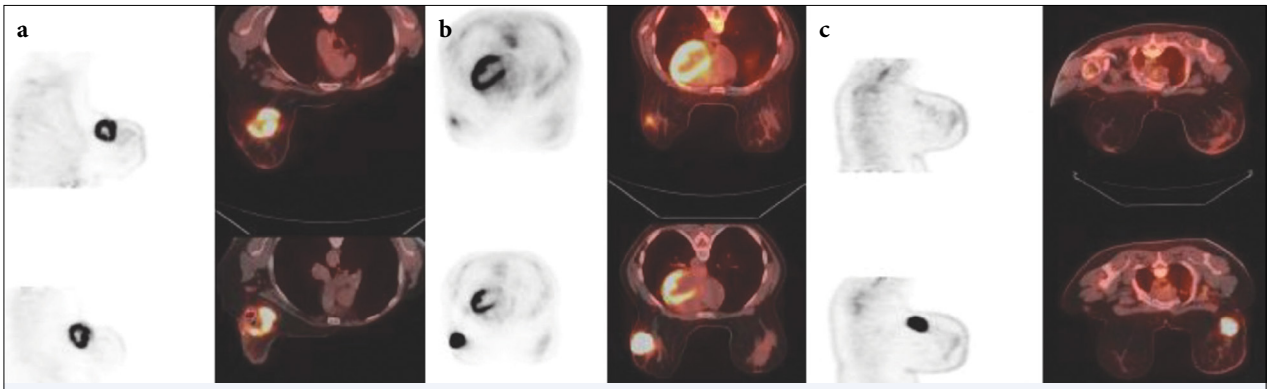

Fig. 2. (a-c) Fifty-seven years old, left breast invasive ductal carcinoma, Grade 3, TN, baseline PET/CT (bottom row) tumor size 65×62×55 mm, SUV_{max}: 18.6. After two cycles of chemotherapy, the tumor size decreased to 38×43×42 mm and SUV_{max} to 11.2 on PET/CT (upper row) (a), 43 years old, left invasive ductal carcinoma, Grade 3, TN, baseline PET/CT (bottom row) tumor size 40×33×38 mm, SUV_{max}: 21.2, tumor size regressed to 15×14×9 mm and SUV_{max}: 2 after two cycles of chemotherapy (upper row) (b), 54 years old, right breast invasive ductal carcinoma, Grade 3, ER-, PR-, HER2+, tumor size in baseline PET/CT (bottom row) 47×35×41 mm, SUV_{max}: 16.7, tumor completely disappeared after two cures of chemotherapy (upper row). Surgical outcome: No residual tumor was observed (c).
PET/CT: Positron emission tomography/Computed tomography; TN: Triple negative; ER: Estrogen receptor; PR: Progesterone receptor; HER2: Human epidermal growth factor receptor-2.

pendent predictor in multivariate analysis.[23] In our study, the baseline PSI, % PSI change, and % SV change from MRI parameters differed in PCR and non-pCR groups. The highest predictive value among these parameters is % SV. Volume change was correlated with metabolic parameters, and the highest correlation was found between % MTV-adp and % TLG-adp. In addition, it has been reported that hybrid ^{18}F-FDG PET/MRI imaging may provide more satisfactory results than ^{18}F-FDG PET and MRI for the early assessment of NAC response in patients with breast cancer.[30]

Limitations

Although the study started with 46 patients, we had to exclude some patients due to a lack of data. Our study group was heterogeneous as the response differed according to the receptor groups. Separate statistical evaluation according to receptor subgroups could not be made due to the low number of patients.

Table 4 Table showing the sensitivity, specificity, positive-negative predictive, and accuracy values calculated for the ^{18}F-FDG PET/CT and MRI parameters and the threshold value, whose p-value was significant in the ROC analysis

Parameter	AUC	95 CI%	p	Threshold	Sensitivity	Specificity	PPV	NPV	Accuracy
MRI parameters									
Peak signal intensity	0.794	0.651-0.937	0.007	250.5	70	69.2	50	85.7	71.4
Baseline PET/CT parameters									
SUV_{max}	0.801	0.659-0.942	0.003	10.34	75	75	56	87.5	75
SUL_{peak}	0.804	0.663-0.944	0.003	5.41	75	67.9	50	86.36	70
TLG-adp	0.717	0.553-0.881	0.031	64.5	75	64.3	47.36	85.7	67.5
MRI parameters % change									
Peak signal intensity	0.771	0.589-0.954	0.03	-34.92	71.4	80	50	90.9	78
Spherical volume	0.829	0.672-0.985	0.009	-64.49	80	73.1	53.3	90.4	75
PET/CT parameters % change									
SUL_{peak}	0.740	0.540-0.940	0.039	-72.82	66.7	81.8	60	85.7	77.4
MTV-adp	0.790	0.595-0.986	0.012	-73.04	77.8	86.4	70	90.5	83.8
TLG-adp	0.785	0.590-0.981	0.014	-88.21	77.8	81.8	63.6	90	80.6

FDG PET/CT: FDG positron emission tomography/Computerised tomography; MRI: Magnetic resonance imaging; ROC: Receiver operating characteristic curve; AUC: Area under the curve; CI: Confidential interval; PPV: Positive predictive value; NPV: Negative predictive value; SUL_{peak} corresponding to the highest possible mean value of a 1 cm^3 spherical volume of interest (VOI); TLG-adp: Total lesion glycolysis with adaptive SUV threshold method; MTV-adp: Metabolic tumor volume with adaptive SUV_{max} threshold method

Turk J Oncol 2022;37(4):426–35
doi: 10.5505/tjo.2022.3701

CONCLUSION

Late prone imaging is successful in evaluating breast tumors; therefore, late imaging should be used in the late period in addition to standard whole-body imaging. Percentage changes in SV, MTV, and TLG can identify non-responding patients better than other parameters. There is no standard for when interim imaging to predict NAC response.

Peer-review: Externally peer-reviewed.

Conflict of Interest: All authors declared no conflict of interest.

Ethics Committee Approval: The study was approved by the Hacettepe University Non-interventional Clinical Research Ethics Committee (no: GO 13/45-29, date: 23/01/2013).

Financial Support: None declared.

Authorship contributions: Concept – M.T., M.G.A., K.A., F.B.D., B.E.; Design – O.K., M.T., P.Ö.K., M.G.A., K.A., F.B.D., B.E.; Supervision – M.T., F.B.D., B.E.; Funding – None; Materials – None; Data collection and/or processing – M.T., P.Ö.K., M.G.A., K.A., F.B.D., B.E.; Data analysis and/or interpretation – O.K., M.T., B.E.; Literature search – O.K., M.T., K.A., B.E.; Writing – O.K., M.T., K.A., F.B.D., B.E.; Critical review – O.K., M.T., P.Ö.K., M.G.A., K.A., F.B.D., B.E.

REFERENCES

1. Wolff AC, Davidson NE. Primary systemic therapy in operable breast cancer. J Clin Oncol 2000;18(7):1558–69.
2. Fayanju OM, Ren Y, Thomas SM, Greenup RA, Plichta JK, Rosenberger LH, et al. The clinical significance of breast-only and node-only pathologic complete response (pCR) after neoadjuvant chemotherapy (NACT): A review of 20,000 breast cancer patients in the National Cancer Data Base (NCDB). Ann Surg 2018;268(4):591–601.
3. Buzdar AU, Ibrahim NK, Francis D, Booser DJ, Thomas ES, Theriault RL, et al. Significantly higher pathologic complete remission rate after neoadjuvant therapy with trastuzumab, paclitaxel, and epirubicin chemotherapy: results of a randomized trial in human epidermal growth factor receptor 2-positive operable breast cancer. J Clin Oncol 2005;23(16):3676–85.
4. Imbriaco M, Caprio MG, Limite G, Pace L, De Falco T, Capuano E, et al. Dual-time-point ^{18}F-FDG PET/CT versus dynamic breast MRI of suspicious breast lesions. AJR Am J Roentgenol 2008;191(5):1323–30.
5. Malhotra A, Tincey S, Naidu V, Papagiorcopulo C, Ghosh D, Tan PH, et al. Characterisation of MRI indeterminate breast lesions using dedicated breast PET and prone FDG PET-CT in patients with breast cancer-a proof-of-concept study. J Pers Med 2020;10(4):148.
6. Abramson RG, Lambert KF, Jones-Jackson LB, Arlinghaus LR, Williams J, Abramson VG, et al. Prone versus supine breast FDG-PET/CT for assessing locoregional disease distribution in locally advanced breast cancer. Acad Radiol 2015;22(7):853–9.
7. Fowler AM, Mankoff DA, Joe BN. Imaging neoadjuvant therapy response in breast cancer. Radiology 2017;285(2):358–75.
8. Schmitz AMT, Teixeira SC, Pengel KE, Loo CE, Vogel WV, Wesseling J, et al. Monitoring tumor response to neoadjuvant chemotherapy using MRI and ^{18}F-FDG PET/CT in breast cancer subtypes. PLos One 2017;12(5):e0176782.
9. Gu YL, Pan SM, Ren J, Yang ZX, Jiang GQ. Role of magnetic resonance imaging in detection of pathologic complete remission in breast cancer patients treated with neoadjuvant chemotherapy: a meta-analysis. Clin Breast Cancer 2017;17(4):245–55.
10. Pahk K, Kim S, Choe JG. Early prediction of pathological complete response in luminal B type neoadjuvant chemotherapy-treated breast cancer patients: comparison between interim ^{18}F-FDG PET/CT and MRI. Nucl Med Commun 2015;36(9):887–91.
11. Edge SB, Compton CC. The American Joint Committee on Cancer: the 7th edition of the AJCC cancer staging manual and the future of TNM. Ann Surg Oncol 2010;17(6):1471–4.
12. Cortazar P, Zhang L, Untch M, Mehta K, Costantino JP, Wolmark N, et al. Pathological complete response and long-term clinical benefit in breast cancer: the CTNeoBC pooled analysis. Lancet 2014;384(9938):164–72.
13. Mazouni C, Peintinger F, Wan-Kau S, Andre F, Gonzalez-Angulo AM, Symmans WF, et al. Residual ductal carcinoma *in situ* in patients with complete eradication of invasive breast cancer after neoadjuvant chemotherapy does not adversely affect patient outcome. J Clin Oncol 2007;25(19):2650–5.
14. Guarneri V, Broglio K, Kau SW, Cristofanilli M, Buzdar AU, Valero V, et al. Prognostic value of pathologic complete response after primary chemotherapy in relation to hormone receptor status and other factors. J Clin Oncol 2006;24(7):1037–44.
15. Kupik O, Akin S, Tuncel M, Eren G, Türker A, Kars A, et al. Comparison of clinical and PET-derived prognostic factors in patients with non-Hodgkin lymphoma: a special emphasis on bone marrow involvement. Nucl Med Commun 2020;41:540–9.
16. Moy L, Ponzo F, Noz ME, Maguire GQ Jr, Murphy-Walcott AD, Deans AE, et al. Improving specificity of

breast MRI using prone PET and fused MRI and PET 3D volume datasets. J Nucl Med 2007;48(4):528–37.
17. Schillaci O. Use of dual-point fluorodeoxyglucose imaging to enhance sensitivity and specificity. Semin Nucl Med 2012;42(4):267–80.
18. Humbert O, Berriolo-Riedinger A, Riedinger JM, Coudert B, Arnould L, Cochet A, et al. Changes in ^{18}F-FDG tumor metabolism after a first course of neoadjuvant chemotherapy in breast cancer: influence of tumor subtypes. Ann Oncol 2012;23(10):2572–7.
19. Groheux D, Giacchetti S, Hatt M, Marty M, Vercellino L, de Roquancourt A, et al. HER2-overexpressing breast cancer: FDG uptake after two cycles of chemotherapy predicts the outcome of neoadjuvant treatment. Br J Cancer 2013;109(5):1157–64.
20. Andrade WP, Lima EN, Osório CA, do Socorro Maciel M, Baiocchi G, Bitencourt AG, et al. Can FDG-PET/CT predict early response to neoadjuvant chemotherapy in breast cancer? Eur J Surg Oncol 2013;39(12):1358–63.
21. Lee SM, Bae SK, Kim TH, Yoon HK, Jung SJ, Park JS, et al. Value of ^{18}F-FDG PET/CT for early prediction of pathologic response (by residual cancer burden criteria) of locally advanced breast cancer to neoadjuvant chemotherapy. Clin Nucl Med 2014;39(10):882–6.
22. Hatt M, Groheux D, Martineau A, Espié M, Hindié E, Giacchetti S, et al. Comparison between ^{18}F-FDG PET image-derived indices for early prediction of response to neoadjuvant chemotherapy in breast cancer. J Nucl Med 2013;54:341–9.
23. Tateishi U, Miyake M, Nagaoka T, Terauchi T, Kubota K, Kinoshita T, et al. Neoadjuvant chemotherapy in breast cancer: prediction of pathologic response with PET/CT and dynamic contrast-enhanced MR imaging--prospective assessment. Radiology 2012;263(1):53–63.
24. Wang Y, Zhang C, Liu J, Huang G. Is ^{18}F-FDG PET accurate to predict neoadjuvant therapy response in breast cancer? A meta-analysis. Breast Cancer Res Treat 2012;131(2):357–69.
25. Mghanga FP, Lan X, Bakari KH, Li C, Zhang Y. Fluorine-18 fluorodeoxyglucose positron emission tomography-computed tomography in monitoring the response of breast cancer to neoadjuvant chemotherapy: a meta-analysis. Clin Breast Cancer 2013;13(4):271–9.
26. Humbert O, Berriolo-Riedinger A, Cochet A, Gauthier M, Charon-Barra C, Guiu S, et al. Prognostic relevance at 5 years of the early monitoring of neoadjuvant chemotherapy using (18)F-FDG PET in luminal HER2-negative breast cancer. Eur J Nucl Med Mol Imaging 2014;41(3):416–27.
27. Bolouri MS, Elias SG, Wisner DJ, Behr SC, Hawkins RA, Suzuki SA, et al. Triple-negative and non-triple-negative invasive breast cancer: association between MR and fluorine 18 fluorodeoxyglucose PET imaging. Radiology 2013;269(2):354–61.
28. Pengel KE, Koolen BB, Loo CE, Vogel WV, Wesseling J, Lips EH, et al. Combined use of ^{18}F-FDG PET/CT and MRI for response monitoring of breast cancer during neoadjuvant chemotherapy. Eur J Nucl Med Mol Imaging 2014;41(8):1515–24.
29. Lim I, Noh WC, Park J, Park JA, Kim HA, Kim EK, et al. The combination of FDG PET and dynamic contrast-enhanced MRI improves the prediction of disease-free survival in patients with advanced breast cancer after the first cycle of neoadjuvant chemotherapy. Eur J Nucl Med Mol Imaging 2014;41(10):1852–60.
30. Bruckmann NM, Morawitz J, Fendler WP, Ruckhäberle E, Bittner AK, Giesel FL, et al. A role of PET/MR in breast cancer? Semin Nucl Med 2022;52(5):611–8.